Speed-Sensorless AC Drives With the Rotor Time Constant Parameter Update

Darko P. Marčetić, *Member, IEEE*, and Slobodan N. Vukosavić, *Member, IEEE*

***Abstract*—This paper presents a new technique for online identification of an induction motor rotor time constant. The technique is designed for a shaft-sensorless indirect field-oriented control induction motor drive with a model reference adaptive system (MRAS)-based speed estimator. The MRAS estimator is sensitive to the changes in the rotor time constant, and online identification of that parameter is essential. If rotor parameter error exists, it does not only change the achieved rotor speed, but it also changes the dynamic behavior of the whole field control and speed estimation structure. The proposed rotor parameter update is exactly based on the newly introduced dynamic model of the potentially detuned MRAS-based speed estimator. The technique avoids the use of test signals and rather extracts the needed information from the ever-present signal jitter, which is inherent to the current and speed servo loops. This paper demonstrates that the phase angle difference between some spectral components of selected small signals within the speed estimator can be used for rotor parameter update. Computer simulations and experiments are performed under a variety of conditions to validate the effectiveness of the proposed rotor parameter update technique.**

***Index Terms*—AC motor drives, model reference adaptive control, parameter estimation.**

I. Introduction

HIGH-PERFORMANCE servo applications of an induction motor can be made possible by implementing the vector control technology. This advance in control technology, coupled with consistent price reduction in power electronics, made the vector-controlled induction motor highly competitive on the low-cost motor system market. Further advance in the induction motor drive technology is also feasible, and it is coupled with the elimination of the sensors needed for the drive to operate. In particular, the development of a shaft-sensorless induction drive is the best answer for the persistent demand from the market place for less expensive and yet more robust drives. However, in applications where the safety regulations apply, shaft-sensorless operation is acceptable only in cases where a robust reliable speed estimation is available, not being prone to thermal drift or any other secondary effect that may endanger correct speed estimation.

Currently, there are two parallel paths toward a robust sensorless solution [1]. Two competing technologies are the machine model-based schemes and the schemes using test signal to exploit the anisotropic properties of machine. The introduction of test signal keeps machine observable even when rotor-induced voltage approaches zero. Uses of different machine anisotropies are reported, such as magnetic saturation or rotor slotting [2] or rotor slot openings modified in sinusoidal pattern [3]. Alternatively, model-based sensorless algorithms using full observer approach, upgraded with online parameter identification algorithms, are also capable of operating at very low rotor speeds [4]–[6]. However, vast majority of speed-sensorless drives are used in low-cost drive applications, without the need to operate at standstill. For these applications, calculation-intensive algorithms associated with high-end processor using expensive peripherals and power supply should be avoided. In [7], Schauder investigates the rotor flux-based model reference adaptive system (MRAS) for speed estimation in drives with indirect field-oriented control (IFOC). The method is rather simple to implement and uses minimum processor time and memory. Still, the major drawback of MRAS is the open-loop flux estimator sensitive to an error in terminal voltage estimation and integration, as well to an error in stator resistance parameter R_s. Listed problems with the reference model can be significantly reduced [8], [9]. Nevertheless, the sensitivity of the adjustable model used in MRAS to an error in the rotor circuit parameters must also be considered. In particular, if the rotor time constant parameter T_r^* is not equal to its actual value T_r, an error in the estimated rotor speed will be introduced. The problem gets more significant in the low-rotor-speed region, where it becomes essential to upgrade the speed estimator with an online T_r identification mechanism.

Variation of T_r is caused mainly by the change in rotor resistance due to temperature and also by the change in rotor inductance due to saturation. Saturation-induced variation in actual T_r value does not need to be tracked, but rather, it can be predicted and included in the feedforward flux model [10]. However, slow-tracking T_r^* update algorithm is still required for online compensation of unpredictable T_r thermal drift.

The research for online T_r identification mechanism starts for IFOC drives using shaft sensor. In those drives, an error in T_r^* greatly affects an open-loop slip estimator and leads to undesirable cross coupling and deterioration of overall drive performance. This sensitivity is well recognized in the literature, and different T_r identification mechanisms are reported [11]. Two basic approaches were used: the schemes with injected test signals [12] and those without injected test signals.

Manuscript received April 6, 2007.
D. P. Marčetić is with the Faculty of Technical Sciences, University of Novi Sad, 21000 Novi Sad, Serbia (e-mail: darmar@uns.ns.ac.yu; darko.marcetic@eacemr.com).
S. N. Vukosavić is with the Faculty of Electrical Engineering, University of Belgrade, 11000 Belgrade, Serbia.
Color versions of one or more of the figures in this paper are available online at http://ieeexplore.ieee.org.
Digital Object Identifier 10.1109/TIE.2007.899880

Most methods from the second group employ MRAS parameter update using different motor states or outputs: stator voltages [13], reactive power [14], or special rotor flux-based criterion function [15] insensitive to R_s thermal drift and/or deadtime error. Also, the algorithm based on sensitivity analysis of the recursive leakage inductance estimation was reported in [16]. The fourth-order sliding-mode flux observer allowing $1/T_r$ identification is proposed in [17]. A rather different approach using drives transient stage for $1/T_r$ update is reported in [18].

In the case of the shaft-sensorless drives, the T_r identification problem is almost completely overshadowed by the stator circuit parameter drift and other reference flux estimation problems. The first reason for it is the higher sensitivity of sensorless schemes to stator circuit parameter error. The second is the complexity of the problem. Parallel estimation of rotor speed and rotor time constant in IFOC drive is possible only if rotor flux varies, which is not the case in steady state [19]. One way to separate rotor parameter error from rotor speed is the use of test signal, keeping the drive in transient state. The authors in [6] suggest superimposed two ac components in the field current. However, avoiding the unwanted test signal is the best path toward the optimal parameter estimation solution. Akatsu and Kawamura [19] show that test signals are not necessary and recommend the usage of speed transients, always accompanied with the rotor flux change. The authors use the least mean square algorithm, updating the rotor resistance value only when enough information is available. This method cannot be used around a constant speed, and the converging time of the algorithm varies with amplitude of available signal. Using a different approach, the authors in [25] estimate the rotor speed in an open-loop manner, using motor state equations corrected with online updated R_s and R_r. Rotor parameter is estimated using available speed estimates within MRAS having artificial neural network instead of current rotor flux model.

The aim of this paper is to introduce a new possible source of information for the T_r identification, which is suitable for use in IFOC speed-sensorless ac drive. First, we refer to the MRAS-based speed estimator proposed in [7]. In Section III, the small-signal dynamics of a detuned sensorless drive is closely analyzed. The work is done to find the useful information about the error in T_r^*. It is assumed that the values of T_r^* that are used in the slip calculator and in the MRAS estimator are equal, but they not accurate. As a result, new elements were added to the small-signal propagation model. Section IV presents the novel algorithm based on the small-signal model of a detuned MRAS-based speed estimator. The algorithm achieves online correction of T_r^* based on the phase delay between some spectral components of the q stator current and the first derivative of MRAS speed estimator error. It is tested using computer simulations, and the results are presented. Finally, via practical experiments using inherent small-signal jitter, the usefulness of suggested technique is demonstrated.

II. MRAS Speed Estimator

The speed estimation based on the MRAS makes use of two machine models with different structures that estimate the same motor state. The primary used state variable is the rotor flux vector. The reference voltage and the adjustable current rotor flux models are given in (1) and (2). The error signal used to tune estimated speed is the phase angle between two vectors (3). Thus

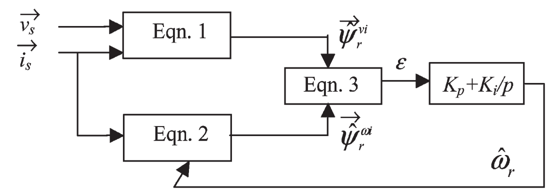

Fig. 1. Block diagram of MRAS-based speed estimator.

$$p\begin{bmatrix}\psi_{\alpha r}^{vi}\\ \psi_{\beta r}^{vi}\end{bmatrix} = \frac{L_r}{L_m}\left(\begin{bmatrix}v_{\alpha s}\\ v_{\beta s}\end{bmatrix} - \begin{bmatrix}R_s+\sigma L_s p & 0\\ 0 & R_s+\sigma L_s p\end{bmatrix}\begin{bmatrix}i_{\alpha s}\\ i_{\beta s}\end{bmatrix}\right) \tag{1}$$

$$p\begin{bmatrix}\psi_{\alpha r}^{\omega i}\\ \psi_{\beta r}^{\omega i}\end{bmatrix} = \begin{bmatrix}-\frac{1}{T_r} & -\omega_r\\ \omega_r & -\frac{1}{T_r}\end{bmatrix}\begin{bmatrix}\psi_{\alpha r}^{\omega i}\\ \psi_{\beta r}^{\omega i}\end{bmatrix} + \frac{L_m}{T_r}\begin{bmatrix}i_{\alpha s}\\ i_{\beta s}\end{bmatrix} \tag{2}$$

$$\varepsilon = \psi_{\alpha r}^{\omega i}\psi_{\beta r}^{vi} - \psi_{\beta r}^{\omega i}\psi_{\alpha r}^{vi} \tag{3}$$

where $\vec{\psi}_r^{vi} = [\psi_{\alpha r}^{vi} \quad \psi_{\beta r}^{vi}]^T$, $\vec{\psi}_r^{\omega i} = [\psi_{\alpha r}^{\omega i} \quad \psi_{\beta r}^{\omega i}]^T$, $\vec{v}_s = [v_{\alpha s} \quad v_{\beta s}]^T$, and $\vec{i}_s = [i_{\alpha s} \quad i_{\beta s}]^T$ are outputs of the rotor flux voltage model, current model, stator voltages, and currents, respectively. All variables are in a two-axis stationary reference frame. ω_r is the rotor angular frequency; L_m, L_s, and L_r are the magnetizing, stator, and rotor inductances, respectively; $\sigma = 1 - L_m^2/L_sL_r$ is the total leakage factor; and $p = d/dt$.

The phase difference between two estimated rotor flux vectors is used to tune estimated speed variable and, therefore, to make correction of the model (2) result, as shown in Fig. 1.

The reference voltage model is an open-loop flux estimator and is therefore sensitive to parameter variations, stator voltage estimation, and integration errors. To insure robust work of this structure, the voltage estimation must include all the inverter nonlinearity effects, which are the switching device deadtime and conducting voltage drop [8]. Furthermore, the R_s thermal drift must be compensated [6], [8], [19], [22]. Method [19] corrects R_s^* tracking an error in adjustable flux vector amplitude, and it is most suited for MRAS. The error in σL_s also affects MRAS. For the squirrel cage motor, σL_s can be set offline, whereas for a motor with the closed rotor slots or double squirrel cage, the update proposed in [24] could be used.

MRAS speed estimation also depends on the correct work of the adjustable flux model (2). Both its parameters (L_m^* and T_r^*) must be altered with the change of the main flux saturation level [21]. However, in case of T_r parameter only, the thermal-drift-induced variation must be also addressed. That part of T_r drift cannot be predicted and must be compensated with an online parameter identification mechanism. The optimal solution for T_r^* update is to introduce the feedforward compensation of flux-level-related variations, in parallel with a robust error identification mechanism tracking only slow thermal-drift-originated changes in T_r.

Based on the collection of the previously published papers, the MRAS surrounding parameter update structure is almost completed and well known. However, the part of the aforementioned structure that is still lacking is a mechanism that can detect thermal-induced T_r variations. One of the possible solutions is discussed in the following sections.

III. Dynamic Response of Detuned MRAS Speed Estimator

Since the steady-state equations contain no information about the T_r^* error, the corrective system under consideration is addressing small-signal dynamics as a new possible source of information. Let us consider a sensorless induction motor with T_r. Within the motor drive, the utilized IFOC and MRAS speed estimator use the same T_r^* parameter. The drive is always in transient state or in quasi-steady-state. The change of the rotor speed reference or the change in the mechanical load will force a speed estimator to track a new rotor speed, thereby forcing a speed regulator to react. Even if that is not the case, current regulators are always in quasi-steady-state due to the pulsewidth-modulation (PWM) inverter noise and/or limited number of current analog-to-digital converter (ADC) bits. Furthermore, the interactions between the speed estimator and speed loop sampling can create additional torque jitter and quantization-induced oscillations [23]. Dynamic analysis of these different small signals can be done by linearizing system equations around the chosen steady-state point [7]. The system transfer function describes the dependence between the small MRAS error signal $\Delta\varepsilon$ and the rotor speed, i.e.,

$$\Delta\varepsilon = \frac{\left(\Psi_{dro}^2 + \Psi_{qro}^2\right)\left(p + \frac{1}{T_r}\right)}{\left(p + \frac{1}{T_r}\right)^2 + \omega_{so}^2}\left(\Delta\omega_r - \Delta\hat{\omega}_r\right) \qquad (4)$$

where $\hat{\omega}_r$ is the estimated rotor angular frequency, Δ is the small-signal symbol, and $\vec{\psi}_{ro} = [\psi_{dro} \quad \psi_{qro}]^T$ is the steady-state rotor flux.

Equation (4) is derived with an assumption that T_r is well known. This paper investigates the influence of T_r^* parameter error on the same small-signal dynamic. First, the steady state of the detuned drive ($T_r^* \neq T_r$) was examined using the variables in the rotor flux reference frame. Using the steady-state equation of the adjustable model $\hat{\omega}_{so}\hat{\psi}_{dro} - (1/T_r^*)\hat{\psi}_{qro} = (L_m/T_r^*)I_{qso}$ and the value of calculated slip $\hat{\omega}_{so} = L_m I_{qso}/(T_r^*\hat{\psi}_{dr0})$, one can conclude that the estimated q-axis rotor flux will always be close to zero. If the reference model is correct, due to the MRAS feedback, actual q rotor flux will also be close to zero. However, attained and estimated steady-state slip could differ.

Around any steady-state point, MRAS flux models respond to small-signal changes at their inputs. The dynamics of ideal reference model can be modeled with the adjustable model using the true rotor speed as input and correct T_r as parameter. The reference ($\vec{\psi}_r^{vi} = \vec{\psi}_r$) and detuned adjustable ($\vec{\psi}_r^{\omega i} = \vec{\hat{\psi}}_r$) models are given in (5) and (6), respectively, after linearization, i.e.,

$$p\begin{bmatrix}\Delta\psi_{dr}\\ \Delta\psi_{qr}\end{bmatrix} = \begin{bmatrix}-\frac{1}{T_r} & \omega_{s0}\\ -\omega_{s0} & -\frac{1}{T_r}\end{bmatrix}\begin{bmatrix}\Delta\psi_{dr}\\ \Delta\psi_{qr}\end{bmatrix} + \frac{L_m}{T_r}\begin{bmatrix}\Delta i_{ds}\\ \Delta i_{qs}\end{bmatrix} + \begin{bmatrix}\Psi_{qro}\\ -\Psi_{dro}\end{bmatrix}\Delta\omega_s \qquad (5)$$

$$p\begin{bmatrix}\Delta\hat{\psi}_{dr}\\ \Delta\hat{\psi}_{qr}\end{bmatrix} = \begin{bmatrix}-\frac{1}{T_r^*} & \hat{\omega}_{s0}\\ -\hat{\omega}_{s0} & -\frac{1}{T_r^*}\end{bmatrix}\begin{bmatrix}\Delta\hat{\psi}_{dr}\\ \Delta\hat{\psi}_{qr}\end{bmatrix} + \frac{L_m}{T_r^*}\begin{bmatrix}\Delta i_{ds}\\ \Delta i_{qs}\end{bmatrix} + \begin{bmatrix}\hat{\Psi}_{qr0}\\ -\hat{\Psi}_{dr0}\end{bmatrix}\Delta\hat{\omega}_s \qquad (6)$$

where ω_{so} and $\hat{\omega}_{so}$ are the steady-state values of actual and estimated slip frequency, respectively; $\vec{\hat{\psi}}_{ro} = [\hat{\psi}_{dro} \quad \hat{\psi}_{qro}]^T$ is the steady-state value of the estimated rotor flux; and $\vec{i}_s = [i_{ds} \quad i_{qs}]^T$ is the stator current. All variables are in a two-axis rotating reference frame.

Two models have different T_r and different steady-state slips, and in the event of a small-signal change ($\Delta\omega_r$ or Δi_{qs}), these models should react differently. In the event of q current change ($\Delta i_{qs} \neq 0$), the change in IFOC estimated slip value is

$$\Delta\hat{\omega}_s = \frac{L_m}{T_r^*\hat{\Psi}_{dr0}}\Delta i_{qs}. \qquad (7)$$

Provided that the same T_r^* value is used in MRAS adjustable model, it becomes insensitive to these changes in the q-axis stator current, and the second and third terms in (6) cancel each other. Hence, if there is no change in d-axis current ($\Delta i_{ds} = 0$) or in speed ($\Delta\omega_r = 0$), the change in q current alone does not trigger any change in adjustable flux vector.

On the contrary, for $\Delta i_{qs} \neq 0$ and $T_r^* \neq T_r$, the actual flux reacts differently. The attained slip variations ($\Delta\omega_s$) are followed, which should be seen in rotor flux reference model.

Neglecting the second-order small signals $\Delta\psi_{dr}\Delta\varepsilon_{qr} \approx 0$ and $\Delta\psi_{qr}\Delta\varepsilon_{dr} \approx 0$, where $\Delta\varepsilon_{dr} = \Delta\psi_{dr} - \Delta\hat{\psi}_{dr}$ and $\Delta\varepsilon_{qr} = \Delta\psi_{qr} - \Delta\hat{\psi}_{qr}$, the linearized MRAS error function now becomes

$$\Delta\varepsilon = \psi_{dro}\Delta\varepsilon_{qr} - \psi_{qro}\Delta\varepsilon_{dr} \approx \psi_{dro}\Delta\psi_{qr}. \qquad (8)$$

Based on (5) and the aforementioned discussion, the resulting linearized MRAS error function is given as follows:

$$\Delta\varepsilon = \frac{\Psi_{dro}^2\left(p + \frac{1}{T_r}\right)}{\left(p + \frac{1}{T_r}\right)^2 + \omega_{s0}^2} \times\left(\left(\Delta\omega_r - \Delta\hat{\omega}_r\right) + \frac{L_m}{\Psi_{dro}}\left(\frac{1}{T_r} - \frac{1}{T_r^*}\right)\Delta i_{qs}\right). \qquad (9)$$

The detuned rotor parameter T_r^* obviously introduces an additional feedforward path in the MRAS error model. That

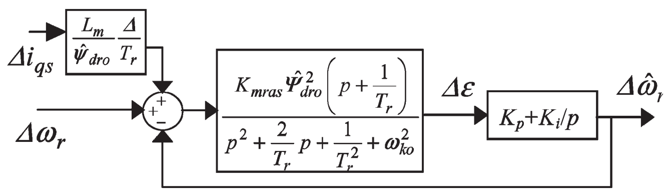

Fig. 2. MRAS estimator dynamics with detuned T_r parameter.

path represents the direct influence of small-signal variations in q stator current (Δi_{qs}) on the actual rotor flux q component. The resulting dynamic model of detuned MRAS is given in Fig. 2.

If the parameter error does exist, additional small-signal propagation will take place via extra-introduced block. However, the same block cancels for $T_r^* = T_r$.

The MRAS feedback, i.e., estimated speed $\hat{\omega}_r$, is a function of MRAS error variable. To further analyze the small-signal dynamics, that closed-loop action must be included, i.e.,

$$\Delta\varepsilon = K(p)\left[\Delta\omega_r + \frac{L_m}{\Psi_{dro}}\left(\frac{1}{T_r} - \frac{1}{T_r^*}\right)\Delta i_{qs}\right],$$

$$K(p) = \frac{K'_{\mathrm{mras}}p\left(p+\frac{1}{T_r}\right)}{p\left(\left(p+\frac{1}{T_r}\right)^2 + \omega_{so}^2\right) + K'_{\mathrm{mras}}\left(pK_p + K_i\right)\left(p+\frac{1}{T_r}\right)} \tag{10}$$

where $K'_{\mathrm{mras}} = K_{\mathrm{mras}}\Psi_{dro}^2$.

The filter action of $K(p)$ depends on the MRAS gains, which can be set for the specified dumping factor ξ and natural angular frequency ω_c [20]. The resulting MRAS closed-loop equation (11) is valid for zero slip condition only, but similar filter action of $K(p)$ is present for any slip frequency, i.e.,

$$\Delta\varepsilon = \frac{K'_{\mathrm{mras}}p}{p^2 + 2\xi\omega_c + \omega_c^2}\left[\Delta\omega_r + \frac{L_m}{\Psi_{dro}}\left(\frac{1}{T_r} - \frac{1}{T_r^*}\right)\Delta i_{qs}\right]. \tag{11}$$

The MRAS error closed-loop transfer function has two independent small-signal inputs: 1) the true rotor speed and 2) the q stator current. The first part of the function describes the MRAS dynamics while tracking an actual rotor speed. The second part is the function of the rotor circuit parameter error and may be used as the source for the parameter correction.

IV. Proposed Estimation Technique

As it is shown in the previous section, the small signal of speed estimator error is the function of the variations in the actual rotor speed $\Delta\omega_r$ and small-signal variations in the q stator current Δi_{qs}. Due to the limited frequency range of machine's mechanical subsystem, it is expected that $\Delta\omega_r$ contains none of the significant high-frequency (HF) components. On the other hand, Δi_{qs} does, and it has a major influence on HF components of the MRAS error signal.

The proposed T_r error identification mechanism uses the relationship between the first derivative of the MRAS estimator

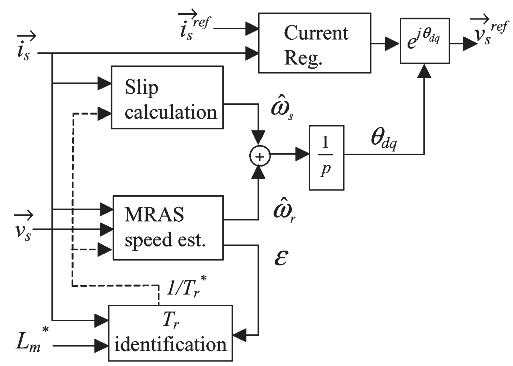

Fig. 3. IFOC with MRAS speed estimator and T_r online identification block.

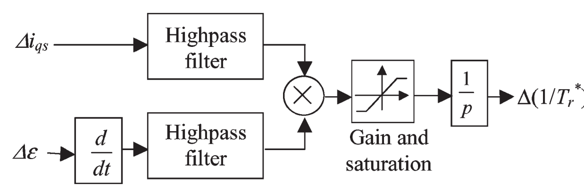

Fig. 4. Simplified block diagram of the proposed $1/T_r$ error estimator.

error $p \cdot \Delta\varepsilon$ and Δi_{qs}, i.e.,

$$p\Delta\varepsilon = \frac{K'_{\mathrm{mras}}p^2}{p^2 + 2\xi\omega_c + \omega_c^2}\left[\Delta\omega_r + \frac{L_m}{\Psi_{dro}}\left(\frac{1}{T_r} - \frac{1}{T_r^*}\right)\Delta i_{qs}\right]. \tag{12}$$

For HF signal components, transfer function (12) has almost constant gain and introduces insignificant signal phase shift. If we also take into consideration that the mechanical rotor speed variations can be neglected for relatively high frequencies, the correlation between the signals Δi_{qs} and $p \cdot \Delta\varepsilon$ can be used to estimate the sign of T_r parameter error, i.e.,

$$p\Delta\varepsilon|_{f\to\infty} \approx K_{\mathrm{mras}}\Psi_{dro}L_m\left(\frac{1}{T_r} - \frac{1}{T_r^*}\right)\Delta i_{qs}. \tag{13}$$

Equation (13) presents the direct link between the sign of the first derivation of the MRAS estimator error signal and the error in the rotor time constant parameter. This connection is valid only for the signal frequencies that are not influenced by the change in the mechanical rotor speed and also are out of the MRAS closed-loop dynamic range.

Figs. 3 and 4 illustrate the $1/T_r^*$ update scheme that is derived from previously presented equations. The estimation block is integrated in IFOC structure with MRAS speed estimator, as shown in Fig. 3. Rotor parameter $1/T_r^*$ is online updated, and its new value is used in MRAS adjustable model as well as in the IFOC slip calculator. The proposed $1/T_r$ error estimation block (Fig. 4) uses multiplication for the phase delay sign extraction. Phase delay sign between the $i_{qs}(t)$ and $p\varepsilon(t)$ signals is then used as the $1/T_r$ error update signal. Integral action forces the parameter error to go to zero. The high-pass filters that are shown are necessary to cancel frequencies that are in MRAS estimator dynamics range and do not depend on T_r^* error only.

The presented technique was initially verified using computer simulations. The model of system in Fig. 3 using T_r^* and a fifth-order induction motor model using T_r are created in

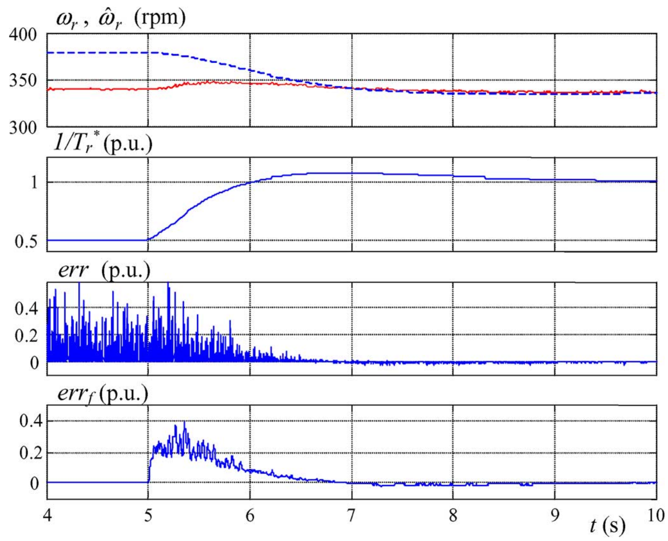

Fig. 5. T_r identification: simulation results for $1/T_r^* = 0.5 * 1/T_r$.

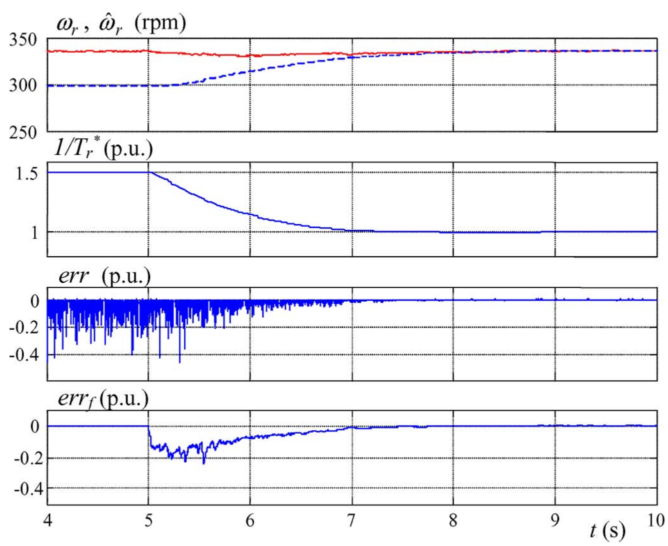

Fig. 6. T_r identification: simulation results for $1/T_r^* = 1.5 * T_r$.

a Matlab/Simulink toolbox. For the parameter update method verification purpose only, the band-limited white noise test signal was added in q stator current signal. Computer simulation results that are shown in Figs. 5 and 6 confirm the functionality of T_r estimator block. The T_r^* parameter was initially set to an incorrect value in both IFOC and MRAS models. Five seconds after the start of the simulation, T_r^* update block was enabled. Simulation results are presented for the rotor speed signal at the motor model output ω_r, estimated rotor speed $\hat{\omega}_r$, updated parameter $1/T_r^*$, phase error signal err, and filtered error signal err_f.

V. Experimental Results

The experimental setup is presented in Fig. 7. The induction motor (rated power 1 kW, rated voltage 195 V, delta connection, two poles, $R_s = 9.1\ \Omega$, $R_r = 5.73\ \Omega$, $L_m = 0.585$ H, $L_s = 0.615$ H, $L_r = 0.615$ H, $\sigma L_s = 0.058$ H, under rated conditions) was loaded with MAGTROL 5410 dynamometer.

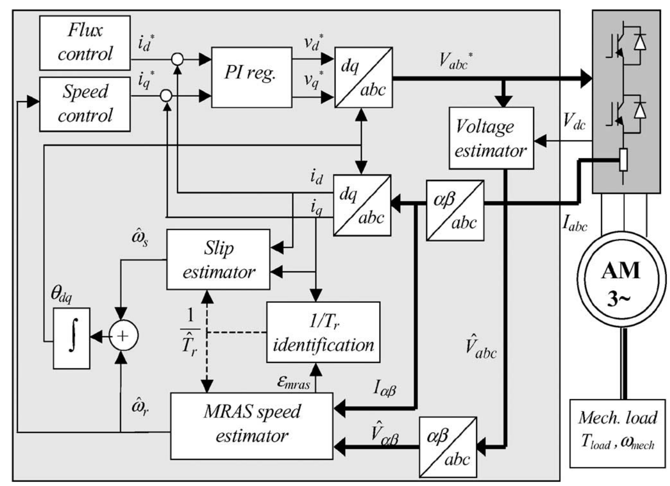

Fig. 7. Experimental setup: shaft-sensorless IFOC with T_r update block.

Three-phase voltage-source inverter was controlled digitally using the low-cost digital signal processor (DSP) ADMC341. Output currents were measured using three shunts placed in inverter legs and further processed using DSP analog front end with bipolar amplifiers and ADC based on the single-slope technique. The rotor speed was monitored via an incremental encoder. The motor voltage was estimated using dc bus samples and the PWM pulses, with the deadtime and conducting voltage drop of switching devices compensated. The PWM frequency was set to 10 kHz, which is the same frequency used to sample inverter leg currents and dc voltage, as well as speed estimator sampling rate. First-order filters $1/(p + \omega_1)$ were used instead of pure integrators to suppress oscillations in estimated flux and MRAS error signals. To maintain the same small-signal dynamic, current signal was processed through $p/(p + \omega_1)$ filters before being used in adjustable model and T_r estimator. To cut off the nonmodeled signal dynamics at HF, bandpass filters were used in T_r estimator instead of high pass. The MRAS closed-loop bandwidth was set to 100 rad/s, which is a relative low frequency range as compared with the current loop actions.

With the feedforward parameter correction present [21], the proposed T_r error estimator was not designed to follow potentially fast flux transients. Consequently, the feedback was enabled only after a stable flux level is reached, with the parameter corrective gains set to relatively low values. In practice, the gains should be set according to an application-specific signal, which is used in the estimation process. In this paper, corrective gains were set experimentally based on the output of a simple phase-sensing algorithm prompted with a specific small signal discovered for the motor in delta connection only.

The rotor speed and flux commands were set to constant values, and small signals in the q stator current were observed. After the rotating transformation has removed the fundamental component from the line current signals, the majority of the q and d stator current signals' energy is contained within the dc and PWM frequency component. However, in the case of motor windings in delta connection, relatively small sixth harmonic was also noticed in line currents, creating matching oscillation in dq frame. Resulting signals for the dq stator currents are

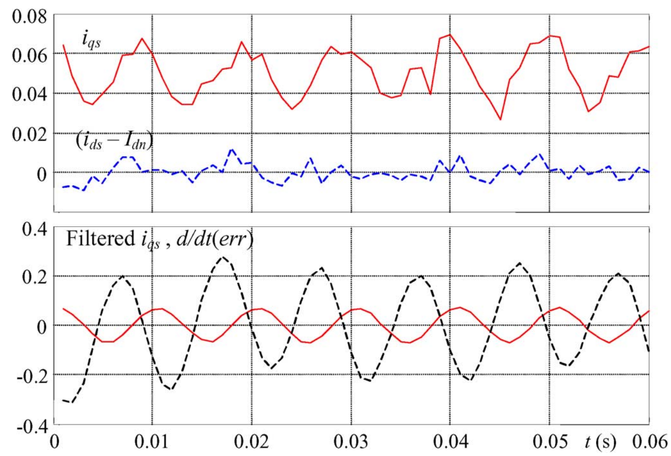

Fig. 8. Small signals utilized for T_r^* online correction. Stator current i_{ds} and i_{qs}, no load. Amplified and bandpass-filtered $d/dt(err)$ and i_{qs} signals.

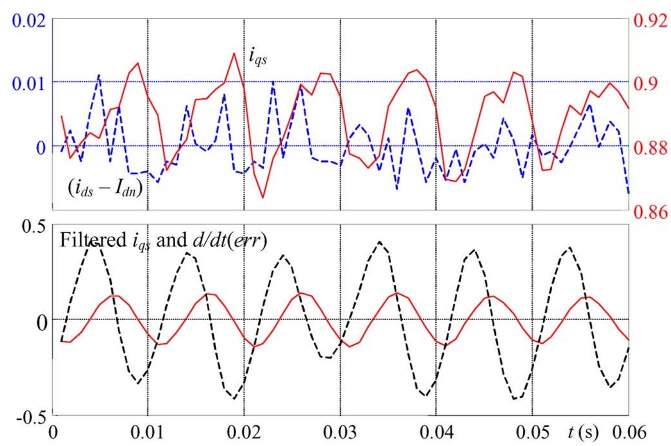

Fig. 9. Small signals utilized for T_r^* online correction. Stator current i_{ds} and i_{qs}, 50% load. Amplified and bandpass-filtered $d/dt(err)$ and i_{qs} signals.

shown on the upper traces of Figs. 8 and 9 for no-load and load conditions, respectively. All presented signals were stored online (1-kHz sampling rate) and then transferred via serial link. Although there is some PWM signal aliasing with each signal, a form of sixth harmonic in q stator current is very clear. It is believed that deadtime that is not compensated in full, presumed windings symmetry during the motor phase current reconstruction, and imperfect current measurement are the root causes for this parasite harmonic.

The discovered small signal has a relatively small amplitude (5% of nominal current value), and there was no observable oscillation in the rotor speed. Similar small signals are acceptable for most of the drive application, provided that their existence does not affect specified output speed and torque range.

Small signal can be separated and amplified using a bandpass filter with the central frequency six times of fundamental. Lower traces show the resulting bandpass-filtered q current and first derivation of MRAS error signal (dashed). As it can be seen, the small signals in q current have corresponding oscillation in the MRAS error signal. The correlation of these two signals can be used for T_r error estimation. Other harmonics of MRAS error signal (first and second), which are present due to

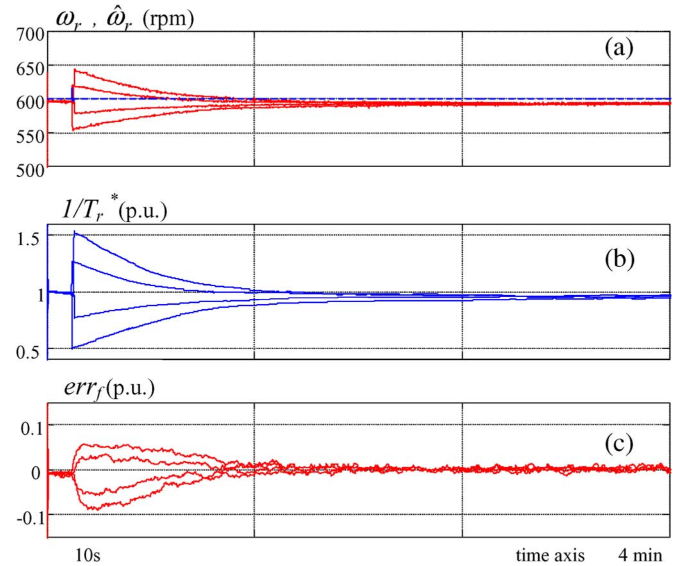

Fig. 10. Speed control mode, 50% rated torque. (a) Measured and estimated (dashed line) speeds. (b) $1/T_r^*$ parameter update. (c) Filtered phase error.

imperfect reference model, can create offset in the T_r^* result and should be canceled with the bandpass filter.

The first experimental result demonstrates the extraction of the parameter error information from the above-described small signal. Fig. 10 shows the T_r identification results for the speed-controlled mode (10 Hz) and dynamometer set for 50% of the nominal load. The nominal rotor flux reference was set. The central frequency of utilized bandpass filters was set to 60 Hz to extract small signal around the chosen rotor speed (600 r/min). Ten seconds after the data acquisition has started, T_r^* was set to incorrect value, i.e., $1/T_r^* = [0.5, 0.75, 1.25, 1.5] \cdot (1/T_r)$. The figure displays the measured and estimated speeds (dashed line), normalized $1/T_r^*$ trace, and filtered phase error signal.

Fig. 10 demonstrates that the small signal that is present in i_{qs} carries enough information for rotor parameter update. The estimator response is slow, but it seems adequate assuming that only the temperature-induced changes in the T_r are tracked.

The next set of experiments explores the algorithm sensitivity to the steady-state point change. Algorithm for the T_r^* update was disabled, and rotor parameter was set to 50% and then to 150% of its nominal value. Parameter update error signal was observed for variety of speed transients and steady speed commands. Taking into account variable frequency of the discovered small signal, during experiments, a bandpass filter with variable central frequency was used. Consequently, similar amount of information about the T_r^* error was available throughout the whole speed range. No-load results (free shaft) are shown in Fig. 11. The estimated (dashed) and measured speeds are displayed on the upper trace, whereas the lower trace shows the T_r estimation error signal. The same signals are shown in Fig. 12 for the motor loaded with 75% of the rated torque.

Experimental results demonstrate that the right information for the parameter update holds for most of the examined operational points. Ones enabled, driven by the displayed error signal, algorithm would correct the T_r^*, and the achieved rotor

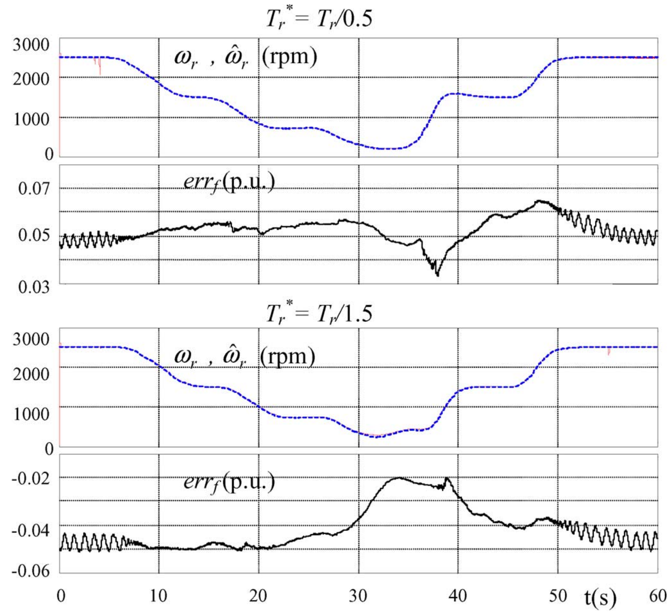

Fig. 11. Different speed transients and operating points, free shaft: 1) measured and estimated (dashed line) rotor speeds and 2) filtered phase error.

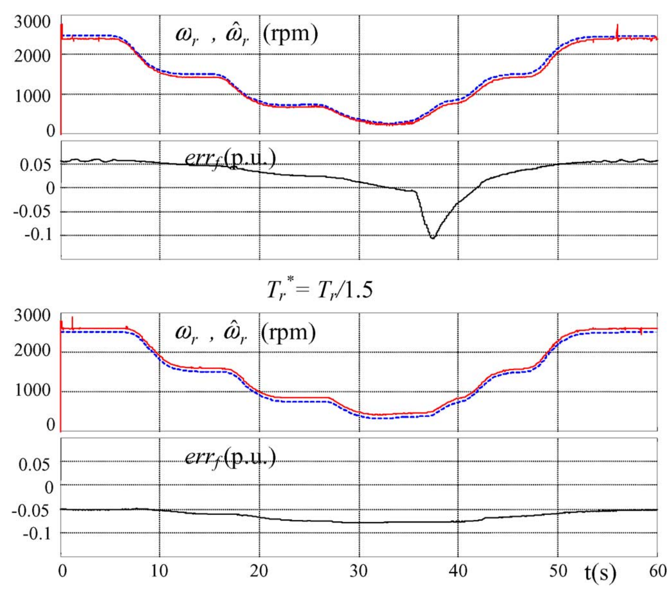

Fig. 12. Different speed transients and operating points, 75% nominal load: 1) measured and estimated (dashed line) rotor speeds and 2) filtered phase error.

speed would match its reference. However, the error in the flux reference increases as the shaft approaches the speeds close to zero, particularly when load is applied. It is noticed that the low shaft speeds together with the applied high load can lead to the sign change in T_r error signal. That would create the unstable feedback, and estimation would fail. This is believed to be the direct result of increased reference flux error.

As it was shown, for accurate work of the proposed T_r identification algorithm, it is required that the MRAS reference model works correctly. That becomes impossible for the rotor speeds very close to zero, and the low speed limit for the algorithm employment must be set. However, additional care must be taken while setting the parameters of the MRAS reference

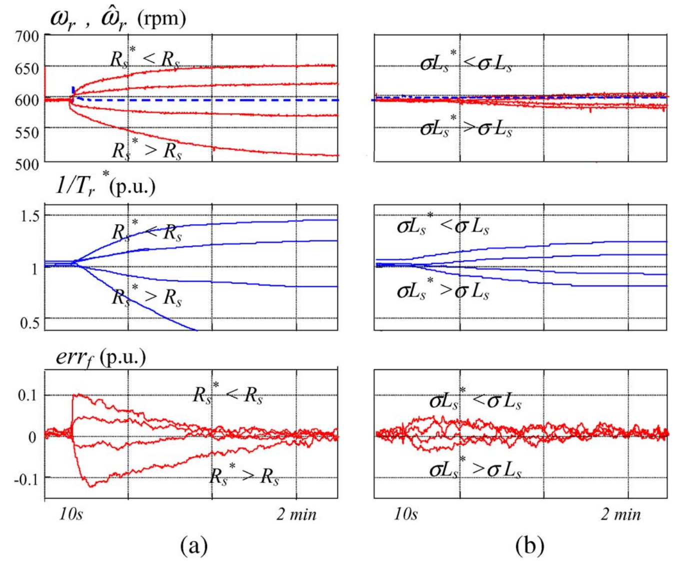

Fig. 13. Speed control mode with T_r update and error in R_s^* and σL_s^*: 1) measured and estimated (dashed line) rotor speeds; 2) $1/T_r^*$ parameter update trace; and 3) filtered phase error.

model. Previously demonstrated experiments were performed with MRAS reference model using correct parameters. The parameters R_s^* and σL_s were estimated while the drive is at rest and kept constant. To role out the change of R_s, the motor temperature was controlled via external ventilation. In addition, in the regular time intervals, R_s^* was validated using the algorithm proposed in [19].

The next set of experiments explores the parameter sensitivity of the T_r update algorithm. Under the scope were possible errors in the parameters R_s^* and σL_s^*. Each parameter was set to the incorrect value, and algorithm operation was observed. Fig. 13(a) shows sensitivity to the R_s variation. Ten seconds after the data acquisition has started, the parameter R_s^* was artificially set to the incorrect value, i.e., $R_s^* = [0.5, 0.75, 1.25, 1.5] \cdot R_s$. Fig. 13(b) shows the influence of the σL_s^* error, i.e., $\sigma L_s^* = [0.8, 0.9, 1.1, 1.2] \cdot \sigma L_{sn}$.

As it was expected (1), the algorithm is sensitive to an error in other MRAS parameters. Wrong flux reference introduces a phase offset, and the parameter T_r^* and, consequently, the speed converge to erroneous values. While sensitivity to the R_s error does not change with load, sensitivity to the σL_s error does, making the method almost insensitive for light loads. It can be also noted that estimation result changes with the voltage estimation error. All of these imperfections affect the reference rotor flux value and introduce unwanted output offset that leads to an error in the estimated T_r.

VI. Conclusion

This paper discusses one technique for online identification of the rotor time constant suitable for speed-sensorless control of induction motor. The proposed parameter correction action is very easy to implement in the already existing MRAS-based speed estimator. Its implementation has the minimum impact on processor power and memory needs. This paper demonstrates that the proposed technique has the potential to eliminate certain drawbacks of the previously published works. It can use various small signals in stator current as an inherent test signal for the rotor parameter update. Although the existing small signals vary and are application specific, these can be found in most sensorless drive applications. Moreover, the advantage of this technique is the use of correlation between two small signals, in selected frequency range, which result can be independent of the steady-state rotor speed and torque. However, the technique does require correct estimation of rotor flux reference vector, which is still an open issue. It is shown that classical reference model can fail if the stator circuit parameters are wrong or if there is an error in stator voltage estimates. The listed problems increase low speed limit for possible use of this technique. Still, better rotor flux estimation schemes are already available, and this technique with some modest modifications may be one possible path toward robust solution for the sensorless rotor circuit parameter update.

References

[1] J. Holtz, "Sensorless control of induction machines—With or without signal injection?" *IEEE Trans. Ind. Electron.*, vol. 53, no. 1, pp. 7–30, Feb. 2006.

[2] C. S. Staines, C. Caruana, G. M. Asher, and M. Sumner, "Sensorless control of induction machines at zero and low frequency using zero sequence currents," *IEEE Trans. Ind. Electron.*, vol. 53, no. 1, pp. 195–206, Feb. 2006.

[3] M. W. Degner and R. D. Lorenz, "Using multiple saliencies for the estimation of flux, position and velocity in AC machines," *IEEE Trans. Ind. Appl.*, vol. 34, no. 5, pp. 1097–1104, Sep./Oct. 1998.

[4] H. Kubota, K. Matsuse, and T. Nakano, "DSP-based speed adaptive flux observer of induction motor," *IEEE Trans. Ind. Appl.*, vol. 29, no. 2, pp. 344–348, Mar./Apr. 1993.

[5] S. Suwankawin and S. Sangwongwanich, "Design strategy of an adaptive full-order observer for speed-sensorless induction-motor drives—Tracking performance and stabilization," *IEEE Trans. Ind. Electron.*, vol. 53, no. 1, pp. 96–119, Feb. 2006.

[6] H. Kubota and K. Matsuse, "Speed sensorless field-oriented control of induction motor with rotor resistance adaptation," *IEEE Trans. Ind. Appl.*, vol. 30, no. 5, pp. 1219–1224, Sep./Oct. 1994.

[7] C. Schauder, "Adaptive speed identification for vector control of induction motors without rotational transducers," *IEEE Trans. Ind. Appl.*, vol. 28, no. 5, pp. 1054–1061, Sep./Oct. 1992.

[8] J. Holtz and J. Quan, "Drift- and parameter-compensated flux estimator for persistent zero-stator-frequency operation of sensorless-controlled induction motors," *IEEE Trans. Ind. Appl.*, vol. 39, no. 4, pp. 1052–1060, Jul./Aug. 2003.

[9] F.-Z. Peng, T. Fukao, and J. S. Lai, "Low speed performance of robust speed identification using instantaneous reactive power for tacholess vector control of induction motors," in *Proc. IEEE Ind. Appl. Soc.*, 1994, pp. 509–514.

[10] E. Levi, S. N. Vukosavić, and V. Vučković, "Study of main flux saturation effects in field oriented induction motor drives," in *Proc. Conf. Rec. IEEE Ind. Electron. Soc. Annu. Meeting, IECON*, 1989, pp. 219–224.

[11] R. Krishnan and A. S. Bharadwaj, "A review of parameter sensitivity and adaptation in indirect vector controlled induction motor drive systems," *IEEE Trans. Power Electron.*, vol. 6, no. 4, pp. 695–703, Oct. 1991.

[12] R. Schmidt, "On-line identification of the secondary resistance of an induction motor in the low-frequency range using a test vector," in *Proc. ICEM*, Pisa, Italy, 1988, pp. 221–225.

[13] T. Rowan, R. Kerkman, and D. Laggate, "A simple on-line adaptation for indirect field orientation of an induction machine," *IEEE Trans. Ind. Appl.*, vol. 27, no. 4, pp. 720–727, Jul./Aug. 1991.

[14] L. Garces, "Parameter adaptation for the speed-controlled static AC drive with a squirrel-cage induction motor operated with variable frequency power supply," *IEEE Trans. Ind. Appl.*, vol. IA-16, no. 2, pp. 173–178, Mar./Apr. 1980.

[15] S. N. Vukosavic and M. R. Stojic, "On-line tuning of the rotor time constant for vector-controlled induction motor in position control applications," *IEEE Trans. Ind. Electron.*, vol. 40, no. 1, pp. 130–138, Feb. 1993.

[16] D. Telford, M. W. Dunnigan, and B. W. Williams, "Online identification of induction machine electrical parameters for vector control loop tuning," *IEEE Trans. Ind. Electron.*, vol. 50, no. 2, pp. 253–261, Apr. 2003.

[17] A. B. Proca and A. Keyhani, "Sliding-mode flux observer with online rotor parameter estimation for induction motors," *IEEE Trans. Ind. Electron.*, vol. 54, no. 2, pp. 716–723, Apr. 2007.

[18] M. W. Degner, J. M. Guerrero, and F. Briz, "Slip-gain estimation in field-orientation-controlled induction machines using the system transient response," *IEEE Trans. Ind. Appl.*, vol. 42, no. 3, pp. 702–711, May/Jun. 2006.

[19] K. Akatsu and A. Kawamura, "Online rotor resistance estimation using the transient state under speed sensorless control of induction motor," *IEEE Trans. Power Electron*, vol. 15, no. 3, pp. 553–560, May 2000.

[20] H. Tajima and Y. Hori, "Speed sensorless field-orientation control of the induction machine," *IEEE Trans. Ind. Appl.*, vol. 29, no. 1, pp. 175–180, Jan./Feb. 1993.

[21] E. Levi and M. Wang, "A speed estimator for high performance sensorless control of induction motors in the field weakening region," *IEEE Trans. Power Electron.*, vol. 17, no. 3, pp. 365–377, May 2002.

[22] E. D. Mitronikas and A. N. Safacas, "An improved sensorless vector-control method for an induction motor drive," *IEEE Trans. Ind. Electron.*, vol. 52, no. 6, pp. 1660–1668, Dec. 2005.

[23] L. Ran and Y. Liao, "Sampling-induced resonance in an encoderless vector-controlled induction motor drive," *IEEE Trans. Ind. Electron.*, vol. 51, no. 3, pp. 551–557, Jun. 2004.

[24] T. Noguchi, S. Kondo, and I. Takahashi, "Field-oriented control of an induction motor with robust on-line tuning of its parameters," *IEEE Trans. Ind. Appl.*, vol. 33, no. 1, pp. 35–42, Jan./Feb. 1997.

[25] B. Karanayil, M. F. Rahman, and C. Grantham, "Online stator and rotor resistance estimation scheme using artificial neural networks for vector controlled speed sensorless induction motor drive," *IEEE Trans. Ind. Electron.*, vol. 54, no. 1, pp. 167–176, Feb. 2007.

Darko P. Marčetić (M'96) was born in Novi Sad, Serbia, in 1968. He received the B.S. degree from the University of Novi Sad, Novi Sad, in 1992 and the M.S. and Ph.D. degrees from the University of Belgrade, Belgrade, Serbia, in 1998 and 2006, respectively.

In the period 2000–2001, he was with the motor company C.E.Set, Italy. In the period 2002–2006, he was with the Motor Technology Center, Emerson Electric, St. Louis, MO, and Emerson Appliance Controls, Elgin, IL, designing low-cost ac drives. Since 2006, he has been with the Faculty of Technical Sciences, University of Novi Sad, where he teaches a course in digital control of electrical drives. His interests are in the areas of ac motor control, system modeling, and machine parameter identification.

Slobodan N. Vukosavić (M'94) was born in Sarajevo, Yugoslavia, in 1962. He received the B.S., M.S., and Ph.D. degrees from the University of Belgrade, Belgrade, Serbia, in 1985, 1987, and 1989, respectively.

He was with Nikola Tesla Institute, Belgrade. He joined the ESCD Laboratory, Emerson Electric, St. Louis, MO, in 1988. In 1991, he was with Vickers Electrics and MOOG Electric, designing motion control products. He is currently a Professor in the Faculty of Electrical Engineering, University of Belgrade, where he serves as the Head of the Department of Power Engineering. He has published extensively and has completed more than 40 large R&D and industrial projects.

Dr. Vukosavić is a member of the Yugoslav National Academy of Engineering. His students won the IEEE IFEC contest in 2005.